

## Nonlinear Excitation of Subcritical Instabilities in a Toroidal Plasma

M. Lesur,<sup>1,\*</sup> K. Itoh,<sup>2,3</sup> T. Ido,<sup>2</sup> M. Osakabe,<sup>2,4</sup> K. Ogawa,<sup>2,4</sup> A. Shimizu,<sup>2</sup> M. Sasaki,<sup>1,3</sup> K. Ida,<sup>2,4</sup> S. Inagaki,<sup>1,3</sup>  
S.-I. Itoh,<sup>1,3</sup> and the LHD Experiment Group<sup>2</sup>

<sup>1</sup>Research Institute for Applied Mechanics, Kyushu University, Kasuga 816-8580, Japan

<sup>2</sup>National Institute for Fusion Science, Toki 509-5292, Japan

<sup>3</sup>Research Center for Plasma Turbulence, Kyushu University, Kasuga 816-8580, Japan

<sup>4</sup>SOKENDAI (The Graduate University for Advanced Studies), Toki 509-5292, Japan

(Received 11 May 2015; published 8 January 2016)

In a collisionless plasma, it is known that linearly stable modes can be destabilized (subcritically) by the presence of structures in phase space. However, nonlinear growth requires the presence of a seed structure with a relatively large threshold in amplitude. We demonstrate that, in the presence of another, linearly unstable (supercritical) mode, wave-wave coupling can provide a seed, which is significantly below the threshold, but can still grow by (and only by) the collaboration of fluid and kinetic nonlinearities. By modeling the subcritical mode kinetically, and the impact of the supercritical mode by simple wave-wave coupling equations, it is shown that this new kind of subcritical instability can be triggered, even when the frequency of the supercritical mode is rapidly sweeping. The model is applied to the bursty onset of geodesic acoustic modes in a LHD experiment. The model recovers several key features such as relative amplitude, time scales, and phase relations. It suggests that the strongest bursts are subcritical instabilities, driven by this mechanism of combined fluid and kinetic nonlinearities.

DOI: 10.1103/PhysRevLett.116.015003

Subcritical instabilities are ubiquitous in fluids and plasmas [1]. These include subcritical, or submarginal, turbulence, which is self-sustained nonlinearly. Subcritical, or submarginal, turbulence is observed in pipe flow, planar Poiseuille flow, and planar Couette flow [2]. In magnetized fusion plasmas, subcritical turbulence is predicted by theory for current-diffusive interchange turbulence [3], and drift-wave turbulence in slab geometry [4]. Subcritical excitation also concerns large-scale perturbations, such as Kelvin-Helmholtz instability [5,6], or the formation of self-sustaining magnetic islands (neoclassical tearing mode) in magnetized fusion plasmas [7].

For this wide range of subcritical systems, the subcritical bifurcation originates from a fluid nonlinearity, or nonlinearity in real space. On the other hand, kinetic nonlinearities, or nonlinearities in the phase space of the particle distribution, play a crucial role in hot plasmas in general. In particular, strong wave-particle resonances lead to the formation of structures in phase space. This is observed in a wide range of laboratory and space plasmas [8]. Theory predicts that these structures can lead to subcritical instabilities, where the kinetic nonlinearity enables the growth of a mode that is linearly damped [9,10]. In this Letter, we report the first theoretical analysis that interprets an experimental observation as a subcritical instability with an essential role of kinetic nonlinearity.

We analyze an intriguing observation in the helical plasma of the LHD, which was described in Ref. [11] (paper 1). Chirping bursts of the energetic particle-driven geodesic acoustic mode (EGAM) [12] are sometimes

accompanied by a stronger burst with twice the amplitude. We call the stronger, faster burst the secondary, or daughter, mode, and the weaker, slower (chirping) EGAM burst the primary, or mother, mode. The daughter's growth rate is 1 order of magnitude larger than the mother's. The amplitude increase of the daughter is so large (compared with the amplitude decrease of the mother) that it clearly violates the Manley-Rowe relations [13]. This suggests that the daughter is not excited by, e.g., simple parametric coupling.

To analyze this observation, we develop a new reduced model, which combines the kinetic description of the daughter mode with the nonlinear fluid coupling [14] between the mother and daughter. This model can be seen as an extension of the Berk-Breizman model [16]. The model is able to qualitatively reproduce relative amplitudes, and time scales, as well as the mother-daughter phase relation. This analysis suggests that the daughter mode is a subcritical instability, which is dormant until the mother excites it by fluid nonlinearity, leveraged by kinetic nonlinearity. Neither fluid nonlinearities alone, nor kinetic nonlinearities alone, can sustain the growth of the daughter mode to large amplitude. Surprisingly, the mechanism involved here is different from that described in earlier theories [17], in that the growth occurs much below the amplitude threshold, and without the dynamical evolution of frequency (chirping).

*Model.*—In a toroidal device, the structure, linear frequency, and linear growth rate of an energetic particle-driven mode are determined by 3D calculations, and evolve on a slow time scale of mean field evolution ( $\sim 100$  ms).

However, the kinetic nonlinear effects, which induce chirping and subcritical instability, happen on a fast time scale ( $\sim 1$  ms) and can be treated perturbatively in a 1D model (the Berk-Breizman model) [18]. Here, we consider the interaction of two modes. To treat the present problem, we split the electric field  $E$  between the two waves  $E = E_1 + E_2$ , and introduce a hybrid model. The daughter mode  $E_1$  is treated by a kinetic 1D model, and the mother mode  $E_2$  is treated as a simple medium for nonlinear energy transfer. For  $E_2$ , we prescribe the initial amplitude  $Z_{2,0}$  and time evolution of frequency  $\omega_2(t)$  from experimental data. We assume that the impact of the mother on the particles near the resonant location of the daughter is negligible. The interaction between the two waves is modeled by the equations for period doubling.

The evolution of the energetic particle distribution  $f(x, v, t)$  in the neighborhood of the resonance of the daughter mode  $E_1$ , is given by a kinetic equation [16,19]

$$\frac{\partial f}{\partial t} + v \frac{\partial f}{\partial x} + \frac{qE_1}{m} \frac{\partial f}{\partial v} = \frac{\nu_f^2}{k_1} \frac{\partial \delta f}{\partial v} + \frac{\nu_d^3}{k_1^2} \frac{\partial^2 \delta f}{\partial v^2}, \quad (1)$$

where  $\delta f \equiv f - f_0$ , and  $f_0(v)$  is the initial velocity distribution. The r.h.s. is a collision operator, where  $\nu_f$  and  $\nu_d$  are input parameters characterizing dynamical friction and velocity-space diffusion, respectively. Here,  $k_1 x$  corresponds to the poloidal angle in the perturbative expansion from 3D to 1D.

The evolution of the two parts of the electric field is given by

$$\begin{aligned} \frac{dZ_1}{dt} = & -\frac{m\omega_p^3}{4\pi q n_0} \int f(x, v, t) e^{-i(k_1 x - \omega_1 t)} dx dv \\ & - \gamma_d Z_1 - i \frac{V}{\omega_1} Z_2 Z_1^* e^{-i\theta t}, \end{aligned} \quad (2)$$

$$\frac{dZ_2}{dt} = -i \frac{V}{\omega_2} Z_1^2 e^{i\theta t}, \quad (3)$$

where  $E_j \equiv Z_j \exp[i(k_j x - \omega_j t)] + \text{c.c.}$ , and  $n_0$  is the total density. The term proportional to  $\gamma_d$  is an external wave damping, which is a model for all linear dissipative mechanisms of the wave energy to the background plasma [16].

Equations (2) and (3) both include a term that describes energy exchange between the mother and daughter. The nonlinear interaction between geodesic acoustic modes (GAMs) (zonal flows) has been studied. Experimentally, direct measurements indicated that GAM can drive energy transfer in a range of frequencies higher than the GAM frequency [20]. In theory, the dominant interaction originates either from second-order coupling between vorticity and parallel velocity, as well as vorticity and density [21], or via higher-order modulation mechanisms of background turbulence [22,23]. In both cases, the coupling takes a

standard form, which depends on the coupling constant  $V$ , and the frequency mismatch  $\theta \equiv \omega_2(t) - 2\omega_1$ . In this model, the linear frequency of the mode,  $\omega_1$  is fixed, but the frequency of  $E_1$  can evolve nonlinearly due to the time evolution of  $Z_1$ .

Equation (3) does not include any dissipation term (no  $\gamma_d$ ) or driving term, because we assume a balance between external drive and external damping for simplicity. This assumption is consistent with the time scale separation between the evolutions of  $E_1$  and  $E_2$ . The time scale of evolution of the mother ( $\sim 10$  ms) is much slower than that of the daughter ( $< 1$  ms), as long as  $|Z_1| < |Z_2|/2$ .

We solve the above model with the COBBLES [24] code. The initial velocity slope is measured by the linear drive  $\gamma_{L,0} = (\pi\omega_1^3)/(2k_1^2 n_0) \partial_v f_0$ . To simulate thermal noise, we add to  $Z_1$  a noise term  $Z_{\text{noise}} e^{i\phi_r}$ , where  $\phi_r$  is a phase that is randomized at each time step.

The system of Eqs. (1) and (2), in the single mode ( $V \rightarrow 0$ ) limit, describes the subcritical excitation of an isolated  $E_1$  [25]. In this case, Landau damping generates a seed phase-space structure, whose growth rate can be positive if the growth due to momentum exchange overcomes the decay due to collisions [17]. This process yields a threshold in initial, or noise, amplitude. With the above multiple-mode model [Eqs. (1)–(3),  $V \neq 0$ ], we are able to investigate whether a large enough seed phase-space structure can originate from the wave energy provided by fluid coupling with a linearly unstable mode. As we will explain, the answer turns out to be no, but subcritical growth can occur anyway.

*Reproducing the experiment.*—We concentrate on the LHD experiment, shot #119729, at  $t \approx 3.88$  s. Figure 1 shows the time evolution of the magnetic perturbations [Fig. 1(a)], and its spectrogram [Fig. 1(b)]. In Fig. 1(a), the signal from the Mirnov coil has been filtered into a low

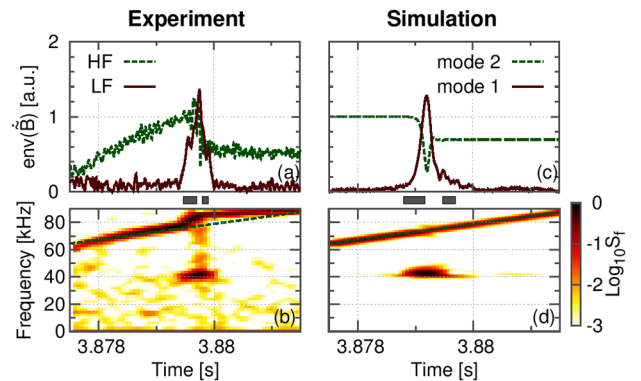


FIG. 1. Comparison between experiment and simulation. (a) Low frequency (LF) and high frequency (HF) components of the magnetic perturbation. Here, “env” refers to the envelope. (b) Spectrogram of the magnetic perturbation. (c) Amplitudes of modes 1 and 2 in the simulation. (d) Spectrogram of the total field. Dashed line in (b) and (d):  $\omega_2(t)$  used as input in the model.

TABLE I. Input parameters of the model. Here,  $Z_0$  is an arbitrary normalizing factor.

Parameter	Value	Range	Independent estimation
$\gamma_{L,0}/\omega_1$	0.03	0.01–0.08	0.1 is supercritical [26]
$\gamma_d/\gamma_{L,0} - 1$	0.03	0.01–0.7	$\gamma_L \approx \gamma_d$ hypothesis
$\nu_f/\gamma_{L,0}$	0.067	0.003–0.3	Fokker-Planck, 0.068
$\nu_d/\gamma_{L,0}$	0.53	0.3–1.5	Fokker-Planck, 0.44
$VZ_0/\omega_1^2$	50	40–80	$\sim 10^{-2}$ – $10^2$ [23]
$Z_{\text{noise}}/Z_{2,0}$	0.06	$10^{-4}$ –0.3	
$10^3 Z_{2,0}/Z_0$	1	0.6–2.0	Input from experimental data
$\omega_1^{-2} d\omega_2/dt$	$5 \times 10^{-4}$	$10^{-4}$ – $10^{-3}$	

frequency (LF,  $f = 30$ – $50$  kHz) component for the daughter mode, and a high frequency (HF,  $f = 60$ – $95$  kHz) component for the mother mode. The dynamical change of frequency of the mother mode (mode 2), around the time of the burst of the daughter mode (mode 1), is modeled as a linear increase. Since the spatial 3D structures of the mother and daughter are very similar [11], we ignore the radial inhomogeneity, and study the ratio between the mother and daughter amplitudes of the magnetic perturbation. To relate the electric field in the simulation to the Mirnov coil signal, we assume a linear relationship between  $|\tilde{\phi}|$  and  $|\tilde{B}|$ , which is consistent with experiment [12].

We scanned the parameter space ( $\gamma_{L,0}, \gamma_d, \nu_f, \nu_d, V$ ). We identified a finite region of the parameter space where the simulation is in qualitative agreement with the experiment, in terms of the time evolution of the amplitude of the perturbed field. Figure 1 shows, for a typical simulation, the time evolution of the amplitudes [Fig. 1(c)], and the spectrogram of the total field [Fig. 1(d)]. Table I lists each input parameter of the simulation (first and second columns). In addition to the time evolution of the amplitude, the simulation agrees qualitatively with the experiment in the sense that the daughter mode is only very slightly chirping ( $\delta\omega/\omega_1 < 10\%$ , as measured by tracking perturbations in the particle distribution), even though a strongly chirping daughter mode is allowed in the model. The lack of chirping of the daughter mode validates, *a posteriori*, our assumption of fixed  $\omega_1$  in the frequency mismatch  $\theta$  used for computing the wave-wave coupling terms.

Furthermore, the mother-daughter phase locking, which was discovered in paper 1, is qualitatively captured by numerical simulations. Figure 2 shows the Lissajous curve during the growth and decay phases, for the experiment [Figs. 2(a) and 2(b)] and for the simulation [Figs. 2(c) and 2(d)] [27]. The mother-daughter phase relation locks itself during the growth phase and the decay phase of the daughter.

Therefore, we have shown that our model is able to qualitatively reproduce the nonlinear evolution of the daughter, in terms of amplitudes, time scales, and phase

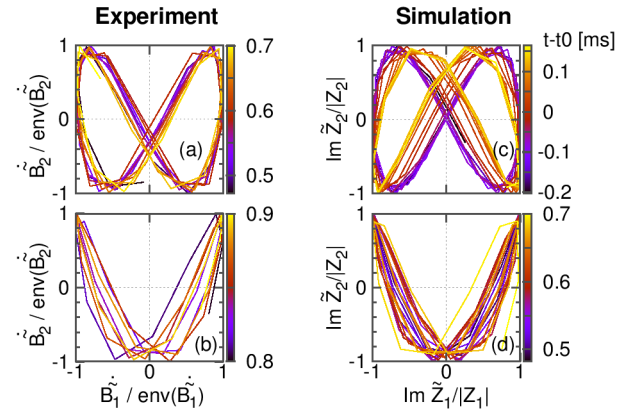


FIG. 2. Lissajous figure during the growth (a) and the decay (b) of the daughter mode in the experiment, and (c),(d) in the simulation. For the simulation,  $\tilde{Z}_i \equiv Z_i e^{-i\omega_i t}$ . The timing is shown by gray rectangles in Fig. 1. Color bars show the time shifted by  $t_0 = 3.879$  s.

locking. Note that we use a simple 1D model that was designed to reproduce qualitatively the excitation mechanism of the daughter. We do not pretend to recover quantitatively from first principles the features of the child, or to reproduce the combined evolution of both the mother and daughter, but rather show the possibility of a new mechanism as follows.

*Collaborative fluid-kinetic nonlinearity.*—Here, we briefly describe the essence of the combined dynamics of two kinds of nonlinear mechanisms. A first crucial point is that, in the limit  $V = 0$ , there is no subcritical instability unless we apply an artificially large initial perturbation  $Z_{1,0} \sim Z_0$ . Therefore, single-mode kinetic nonlinearity alone is insufficient. A second crucial point is that if we remove the kinetic part, that is, the first term of the r.h.s. of Eq. (2), then the amplitude of the daughter stays negligible compared to the amplitude of the mother. Therefore, fluid nonlinearity alone is also insufficient. It is the combination of fluid and kinetic nonlinearities that allows significant subcritical instability. This new hybrid fluid-kinetic subcritical instability is illustrated in Fig. 3, which compares the stability of the daughter without [Fig. 3(a)] and with [Fig. 3(b)] the kinetic term in Eq. (2). The unstable region ( $\max |Z_1|/Z_{2,0} \sim 1$ ) is significantly extended to lower  $V$  in the parameter space of  $(-\gamma, V)$ . Here,  $-\gamma = \gamma_d - \gamma_{L,0}$  is used as a measure of the distance from linear marginal stability.

In previous works [17,24,25], the kinetic subcritical instability was due to the growth of phase-space structures, and thus linked to chirping. Here, chirping does not occur during daughter growth (there is slight chirping, but during daughter decay), consistently with the relatively large  $\nu_d \sim \gamma_{L,0}$  [28]. In fact, the peak amplitude  $|Z_1|$  produced by fluid coupling alone is orders of magnitude below the predicted amplitude threshold for subcritical growth. These observations suggest that the mechanism is different from the previously known kinetic subcritical instability.

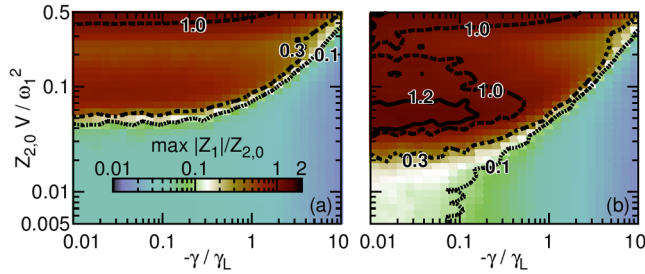


FIG. 3. Nonlinear stability diagram for the daughter mode without (a) and with (b) the kinetic term in Eq. (2). Peak amplitude of the daughter mode as a function of distance from linear stability and the coupling coefficient. The white area is the stability threshold.

Let us give more details about the new mechanism. It is convenient to describe the three terms in the r.h.s. of Eq. (2) as kinetic, dissipative, and coupling terms, respectively. During the daughter growth, the dissipative and coupling terms are nearly locked in antiphase ( $1.2\pi$ – $1.3\pi$  phase difference). Therefore, the coupling acts as an effective reduction of dissipation. The kinetic term is in phase with the dissipative term. In amplitude, all three terms are comparable. Therefore, the sum of the three terms approximately results in a real, positive growth rate  $\sim\gamma_d \sim \gamma_{L,0}$ .

*Impact of input parameters.*—The model includes *a priori* eight input parameters (assuming a constant chirping rate  $d\theta/dt$  for the mother mode at the onset of the daughter mode). Here, we describe the sensitivity, and the experimental and theoretical basis, for these parameters.

We have conducted a sensitivity analysis, where we vary each input parameter, everything else being equal, and measure the impact on the time evolution of the daughter mode. The third column (Range) of Table I lists for each parameter the range (everything else being equal) where the simulation qualitatively agrees with the experiment. Note that the evolution of the daughter mode is mostly sensitive to  $\gamma_{L,0}$ ,  $\nu_d$ ,  $V$ ,  $Z_{2,0}$ , and  $d\omega_2/dt$ .

The fourth column of Table I lists estimations from independent methods when available. Two of the five sensitive parameters,  $Z_{2,0}$ ,  $d\omega_2/dt$ , as well as  $Z_{\text{noise}}$ , are inputs from experimental data. Another sensitive parameter,  $\nu_d$ , as well as  $\nu_f$ , can be obtained from experimental measurements, after projecting the Fokker-Planck collision operator on the resonance surface of the daughter [29,30], including the significant impact of impurities [19]. We use the local plasma parameters around the radial location of the daughter as given in paper 1, and a magnetic shear  $S \approx 0.2$ . In addition, we assume carbon impurities with  $T_C = T_i$  and  $Z_{\text{eff}} = 2$ . We obtain  $\nu_f/\gamma_{L,0} \approx 0.068$  and  $\nu_d/\gamma_{L,0} \approx 0.44$ , which are 1% and 17%, respectively, below the parameters of the simulation shown in Fig. 1.

There remain two parameters with significant impacts: (1) the slope of the energetic particle distribution, parametrized by  $\gamma_{L,0}$ , and (2) the coupling coefficient  $V$ . For (1),

it was shown that the order of magnitude  $\gamma_{L,0}/\omega_1 \sim 0.1$  is relevant for linearly unstable EGAMs on similar LHD plasmas [26], which suggests that 0.03 is relevant for linearly stable EGAMs. For (2), substituting the parameters of the experiment into Eq. (35) of Ref. [23] yields an estimate  $Z_0 V/\omega_1^2 \sim 10^{-2}$ – $10^2$ . The result is sensitive to the radial wave number of the GAM, but not inconsistent with our simulation. Thus,  $V$  is a key parameter, with a finite range that reproduces the experiment, but with a poor theoretical guide. Therefore, the quantitative deduction of  $V$  from the first principles is encouraged.

The model provides the following predictions, which are open to future experimental tests. (1). The ratio between the mother and the daughter mode can become much larger,  $|Z_1|/|Z_2| > 2$ , if the daughter mode exhibits strong chirping,  $\Delta\omega_1 \sim \omega_1$  (see the discussion below). (2). Since the best limit for driving a subcritical instability is  $d\omega_2/dt \rightarrow 0$ , and in this case we observed no nonlinear instability for  $\gamma_d > 2\gamma_{L,0}$ , we predict that there will not appear any subcritical instability with  $\gamma_d \gg \gamma_{L,0}$ .

*Summary.*—We have shown that the model can reproduce key aspects of the experimental observation of paper 1. It interprets the daughter mode as a manifestation of a subcritical instability, driven by the cooperative combination of fluid nonlinearity and kinetic nonlinearity. In contrast with previously known kinetic subcritical instabilities, the amplitude stays below the kinetic threshold, and the chirping of the present fluid-kinetic hybrid subcritical instability seems to be limited by a quasi-phase-matching condition with the mother mode. These results imply a new channel of mode excitation, which modifies the flow of energy in the system.

*Discussion.*—The model underlies a broader phenomenology. By varying the input parameters, it leads to other kinds of nonlinear evolution of both the daughter and the mother mode. In particular, if the ratio  $\nu_f/\nu_d$  increases, the amplitude threshold for pure kinetic instability significantly decreases. For  $\nu_f/\nu_d \sim 1$ , the mother mode can push the daughter mode over the threshold, then the daughter chirps strongly. In this case, the role of the mother is reduced to that of an initial trigger, and the daughter's amplitude can grow an order of magnitude above the mother's amplitude. This may turn out to be a significant issue in the International Thermonuclear Experimental Reactor (ITER), where  $\nu_f/\nu_d$  is predicted to be above unity [30], in contrast to currently operating devices.

In our analysis, we have prescribed the time evolution of the mother frequency  $\omega_2(t)$  with a constant chirping rate. As a caveat, this prescribed evolution ends when  $|Z_1| \sim |Z_2|$ . Indeed, in the experiment, the ratio  $\omega_2/\omega_1$  increases very rapidly, but almost linearly, from 1.9 to 2.0, within a 0.2 ms span during the daughter growth. The model, by its design, is unable to recover this apparent synchronization mechanism. However, the ratio of 2.0 is not reached before the very end of the daughter growth.

This indicates that the synchronization may not be a key aspect of the instability mechanism, although it may be a key aspect of the full dynamics of coupled modes. Reproducing the self-consistent coupled evolution of both the mother and daughter is a relevant challenge that we leave for future work. Here, we focused on the origin of the subcritical, daughter mode.

One of the authors is grateful for stimulating discussions with Y. Kosuga, M. Yagi, H. Wang, M. Kikuchi, K. Miki, and the participants in the Festival de Théorie. This work was supported by grants-in-aid for scientific research of JSPS, Japan (Grants No. 15K18305, No. 15H02155, No. 23244113, and No. 15H02335), by the collaboration programs of the RIAM of Kyushu University and of NIFS, and by the Asada Science Foundation. Computations were performed on the XT system at Kyushu University and Plasma Simulator at NIFS.

---

\*Present address: Institut Jean Lamour, UMR 7198, Lorraine University, 54506 Vandoeuvre-les-Nancy, France.

- [1] A. Yoshizawa, S.-I. Itoh, and K. Itoh, *Plasma and Fluid Turbulence: Theory and Modelling*, (IOP Publishing, Bristol, 2002).
- [2] V. Romanov, *Funct. Anal. Appl.* **7**, 137 (1973).
- [3] M. Yagi, S.-I. Itoh, K. Itoh, A. Fukuyama, and M. Azumi, *Phys. Plasmas* **2**, 4140 (1995).
- [4] J. F. Drake, A. Zeiler, and D. Biskamp, *Phys. Rev. Lett.* **75**, 4222 (1995).
- [5] M. A. Weissman, *Phil. Trans. R. Soc. A* **290**, 639 (1979).
- [6] L. Meignin, P. Gondret, C. Ruyer-Quil, and M. Rabaud, *Phys. Rev. Lett.* **90**, 234502 (2003).
- [7] R. Carrera, R. D. Hazeltine, and M. Kotschenreuther, *Phys. Fluids* **29**, 899 (1986).
- [8] B. Eliasson and P. Shukla, *Phys. Rep.* **422**, 225 (2006).
- [9] T. H. Dupree, *Phys. Fluids* **25**, 277 (1982).
- [10] H. Schamel, *Phys. Plasmas* **19**, 020501 (2012).
- [11] T. Ido *et al.*, preceding Letter, *Phys. Rev. Lett.* **116**, 015002 (2016).
- [12] T. Ido *et al.*, *Nucl. Fusion* **55**, 083024 (2015).
- [13] J. Manley and H. Rowe, *Proc. IRE* **44**, 904 (1956).
- [14] Since the specific mechanism of mode-mode coupling is unknown, we use the vague term of “fluid coupling.” However, we can reasonably speculate that the coupling mechanism belongs to the wide category of parametric-modulational coupling [15].
- [15] R. Z. Sagdeev and A. A. Galeev, *Nonlinear Plasma Theory* (Benjamin, New York, 1969).
- [16] H. L. Berk, B. N. Breizman, and M. Pekker, *Phys. Plasmas* **2**, 3007 (1995).
- [17] M. Lesur and P. H. Diamond, *Phys. Rev. E* **87**, 031101 (2013).
- [18] B. N. Breizman, H. L. Berk, M. S. Pekker, F. Porcelli, G. V. Stupakov, and K. L. Wong, *Phys. Plasmas* **4**, 1559 (1997).
- [19] M. Lesur, Y. Idomura, K. Shinohara, and X. Garbet, *Phys. Plasmas* **17**, 122311 (2010).
- [20] C. Holland, G. R. Tynan, R. J. Fonck, G. R. McKee, J. Candy, and R. E. Waltz, *Phys. Plasmas* **14**, 056112 (2007).
- [21] M. Sasaki, K. Itoh, Y. Nagashima, A. Ejiri, and Y. Takase, *Phys. Plasmas* **16**, 022306 (2009).
- [22] K. Hallatschek and D. Biskamp, *Phys. Rev. Lett.* **86**, 1223 (2001).
- [23] K. Itoh, K. Hallatschek, S.-I. Itoh, P. H. Diamond, and S. Toda, *Phys. Plasmas* **12**, 062303 (2005).
- [24] M. Lesur, Y. Idomura, and X. Garbet, *Phys. Plasmas* **16**, 092305 (2009).
- [25] H. L. Berk, B. N. Breizman, J. Candy, M. Pekker, and N. V. Petviashvili, *Phys. Plasmas* **6**, 3102 (1999).
- [26] H. Wang and Y. Todo, *Phys. Plasmas* **20**, 012506 (2013).
- [27] By comparing the Lissajous diagram between  $\dot{B}$  and  $\text{Im } \tilde{Z}$ , we implicitly assumed a relationship between  $E$  in the 1D model and  $B$  in the 3D model, with a constant, zero phase shift.
- [28] M. Lesur and Y. Idomura, *Nucl. Fusion* **52**, 094004 (2012).
- [29] H. L. Berk, B. N. Breizman, and M. S. Pekker, *Plasma Phys. Rep.* **23**, 778 (1997).
- [30] M. K. Lilley, B. N. Breizman, and S. E. Sharapov, *Phys. Rev. Lett.* **102**, 195003 (2009).